arXiv:cond-mat/0104256v1 [cond-mat.mes-hall] 13 Apr 2001

Multiwalled Carbon Nanotubes as Building Blocks in Nanoelectronics

Markus Ahlskog, Pertti Hakonen, Mikko Paalanen,
Leif Roschier, and Reeta Tarkiainen

Low Temperature Laboratory,
Helsinki University of Technology,
FIN-02015 HUT, Finland

February 1, 2008

Abstract

Molecular level components, like carbon multiwalled nanotubes (MWNT), show great potential for future nanoelectronics. At low frequencies, only the outermost carbon layer determines the transport properties of the MWNT. Due to the multiwalled structure and large capacitive interlayer coupling, also the inner layers contribute to the conduction at high frequencies. Consequently, the conduction properties of MWNTs are not very far from those of regular conductors with well-defined electrical characteristics. In our work we have experimentally utilized this fact in constructing various nanoelectronic components out of MWNTs, such as single electron transistors (SET), lumped resistors, and transmission lines. We present results on several nano- tube samples, grown both using chemical vapor deposition as well as arc-discharge vaporization. Our results show that SET-electrometers with a noise level as low as $6 \cdot 10^{-6}\ e/\sqrt{\mathrm{Hz}}$ (at 45 Hz) can be built using arc-discharge-grown carbon nanotubes. Moreover, short nanotubes with small contact areas are found to work at 4.2 K with good gate modulation. Reactive ion etching on CVD tubes is employed to produce nearly Ohmic components with a resistance of 200 kΩ over a 2 μm section. At high frequencies, MWNTs work over micron distances as special LC-transmission lines with high impedance, on the order of 5 kΩ.

PACS numbers: 73.63.Fg, 73.23.-b, 73.23.Hk

1 INTRODUCTION

The large number of organic compounds and living organisms is based on the unique chemical properties of elemental carbon. Carbon forms a variety of compounds and, in pure form, exists in diamond as well as in graphite structures. Despite these well known properties of carbon, the discovery of fullerenes and nanotubes took the science community by surprise. The carbon nanotubes were discovered by Iijima in 1991 in Japan [1]. It was soon realized that both semiconducting and metallic nanotubes should exist [2]. The mass production of nanotubes succeeded in 1992 [3] and the first electrical transport measurements in 1996 [4]. Various possible applications of nanotubes have quickly emerged, for example in molecular electronics.[5] The Coulomb blockade was detected in transport measurements in 1997,[6, 7] demonstrating that the nanotubes are suitable building blocks of single electron transistors (SETs).

The single electron transistor (SET) has, as an ordinary transistor, three terminals: the source, the drain and the gate. In addition, the SET contains a nearly isolated island between the source and the drain contacts. The principle of the SET is based on the repulsive interaction between electrons which becomes important when the island is smaller than about one micron and its contacts to source and drain are weak (resistance larger than the quantum of resistance $R_Q = h/e^2 \approx 26$ kΩ). The first successful SET was made by Fulton and Dolan[8] at AT&T Bell Laboratories in 1987 using aluminum thin film technology and electron beam lithography. Since the early success with the Aluminum-SET, SETs have also been manufactured out of two-dimensional electron gas of SiMOSFETs, with metal nanoparticles and lately with carbon nanotubes. In case of carbon nanotubes, the nanotube forms the central island and the relatively poor contact resistance between the leads and the nanotube ensures the required isolation.

In this paper we present work on basic electronic devices made of MWNTs. As a building block of a nanoscale electronic device, the carbon nanotube may fill many functions. Here we introduce different cases, based on our own measurements, where a multiwalled carbon nanotube is used either as the island of a SET, as an Ohmic resistor, or as a transmission line. Furthermore, we compare devices made of nanotubes that were synthesized using different methods.

2 BASICS OF NANOTUBES

2.1 Electronic properties

Graphite is made out of fairly loosely connected two dimensional carbon layers, each layer having hexagonal lattice structure. Carbon nanotubes are formed from such graphitic layers.[9] A single walled nanotube (SWNT) is formed when a piece of graphite sheet is wrapped into a cylindrical form, the edges are seamlessly joined together and the ends of the cylinder are closed. A multiwalled nanotube (MWNT) is made out of several concentric graphite cylinders. The SWNTs are about 1-2 nm in diameter. The MWNTs, in contrast, can be as large as 20 - 30 nm in diameter and are more convenient for experiments. In constructing a SWNT one has several possibilities to cut the original graphite sheet: The width and the length of the sheet can be varied as well as the angle between the symmetry axis of the hexagonal sheet and the main axis of the final cylinder. The electrical properties of the nanotube are sensitive to the orientation of the hexagonal lattice because it determines the density of electron states at the Fermi level.

The band structure of graphite was calculated already in 1947 by Wallace using the tight binding approximation[10]. A graphite sheet is a semimetal, whose two-dimensional band structure near the Fermi surface consists of six conical energy surfaces in the first Brillouin zone. Fermi surface of the undoped graphite consists of six points, the vertices of the six cones. When the two dimensional graphite sheet is wrapped into cylindrical form, the transverse electron motion around the cylinder surface becomes quantized. The corresponding transverse energy levels of SWNTs are separated by about 1 eV and only the lowest band is occupied at room temperature and below it. The electrons on the lowest band move along the cylinder axis and behave truly one-dimensionally. One can make nanotubes which are several microns long. The longitudinal quantization of the electron motion leads to the fine structure of the energy bands on the energy scale of 1 meV. This fine structure is, however, washed away by the broadening of the levels due to impurity scattering.

Calculations show that undoped SWNTs are either semiconductors or metals, approximately one third of the tubes having the "metallic" orientation between the underlying hexagonal structure and the tube axis. In the semiconducting nanotubes there are no electron states at the Fermi level and the band gap is several hundreds of meVs. These tubes are good insulators at small bias voltages. In the metallic nanotubes one-dimensional

energy bands cross the Fermi level. They are constructed out of the six energy cones of the graphite. Because three of the cones are equivalent, the six energy cones of graphite collapse into two independent one-dimensional conduction channels. Taking into account the spin degeneracy of the electrons, the metallic SWNTs have altogether four independent conduction channels. The number of conduction channels is important because it determines the electrical conductivity of the nanotube. The conductivity of a ballistic one-dimensional system is given by e^2M/h, where e is the charge of electron, h Planck's constant and M the number of independent conduction channels. Thus the resistance of a ballistic nanotube is expected to be 6.45 kΩ ($M = 4$).

The concentric layers of a MWNT are estimated to be in poor electrical contact to each other. Some experimental results have been interpreted with the assumption that only the outermost layer participates in the electron conduction.[11] Therefore, one expects the electrical properties of the MWNTs and SWNTs to be similar. However, the metallic inner layers can contribute to the electrical properties of the MWNT at high frequencies.[12] In fact, the analysis of tunneling experiments in MWNTs has recently turned out to be more difficult than expected.[13, 14, 15]

2.2 Synthesis of multiwalled carbon nanotubes and their properties

Carbon nanotubes are synthesized with various methods that differ from each other in crucial ways with regard to the growth conditions, resulting in nanotubes of different quality. In MWNTs in particular, various defects can appear that distort the structure of the ideal MWNT. In the arc-discharge[3] (AD) and related methods nanotubes are produced in an inert-gas atmosphere from graphite at such a high local temperature that the carbon evaporates and subsequently forms the nanotubes. Later, catalytical synthesis of nanotubes was started using chemical vapor deposition (CVD) methods [16]. In the CVD technique the nanotubes grow from a catalyst over which a carbon-containing gas is led. The upper temperature is limited by the requirement that the gas is not decomposed by itself. Therefore the growth temperature with the CVD technique is lower than with the other techniques. The lower growth temperature of CVD tubes is considered as the main cause for their more defective structure.

AD tubes are generally straight, as shown in Fig. 1a, and exhibit a rather flawless structure in TEM images. Indeed, these are rather good approxima-

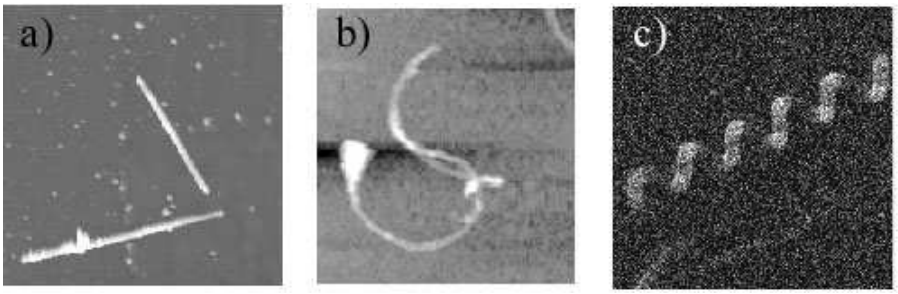

Figure 1: AFM images of typical a) arc-discharge and b) CVD-grown nanotubes. c) SEM image of a CVD-grown helical nanotube (Courtesy of E. Seynaeve, VSM, Kath. Univ. Leuven, Belgium).

tions of the ideal nanotubes whose basic electronic properties were discussed above. Multiwalled CVD tubes, on the other hand, often exhibit a significant amount of disorder in TEM analysis, although images of well ordered sections of individual CVD tubes have also been reported [17]. It is likely that CVD material exhibits large variations in quality. This variation is evident in our experiments on CVD tubes treated with reactive ion etching (RIE). In a short etching time most tubes were uniformly thinned by a factor of 2, while some tubes had vanished almost completely. The defects in a low-quality tube are much more susceptible to an etchant than the regular graphitic walls. As a result of the defective structure, CVD tubes are generally curved when observed either as freestanding in a TEM or as deposited on substrates, as shown in the AFM image of Fig. 1b. This curvature is rigid and often extends into three dimensions. The nanotube (diameter 20 nm) in Fig. 1b has a tail to the left which extends more than 100 nm above the substrate, despite the significant van der Waals forces that exist between the substrate and the nanotube. Note that the tail appears broadened due to the interaction between the AFM tip and the upwards pointing tail section. The most impressive of the three dimensionally extended tubes are the regularly coiled 3D spirals of multiwalled CVD-grown tubes [18], as shown in Fig. 1c. Salvetat *et al.*[19] presented work comparing the elastic moduli of AD and CVD multiwalled tubes, concluding that the former are significantly stiffer than the latter. Thus, although AD tubes have generally better electronic performance from the point of view of device physics, CVD

tubes have their own interesting and useful properties.

3 CONSTRUCTION OF NANOTUBE CIRCUITS

For electronic transport measurements individual nanotubes have to be connected to external leads. This is not a trivial task because the nanotubes are quite small, difficult to image and hard to move around. In making simple nanotube circuits one starts from a solution (actually a dispersion). A droplet of this solution is placed on the substrate at a desired location, and the solvent is evaporated away. This leaves behind a number of randomly placed nanotubes on the surface of the substrate. There are two possibilities to connect the nanotubes to the leads. In the first method the leads are evaporated on top of the nanotubes. This method requires accurate imaging of the nanotubes and sophisticated alignment techniques when making the evaporation mask. In the second method one moves the nanotubes on top of prefabricated gold electrodes (or makes a large array of electrodes in the hope of finding one nanotube already extending over at least two electrodes). Both of these methods are hampered by poor electrical contacts between the nanotubes and electrodes. This is a problem especially in the case, where nanotubes are deposited on top of the electrodes. The contact resistances range from a few tens of kΩ to gigaohms and are not well understood. There are some methods to improve the contacts. Bachtold *et al.* [20] successfully used electron bombardment in SEM, while Jeong-O Lee *et al.*[21] used quick heating at high temperature. We have also used this method in some cases. Contact resistances decrease considerably by a 30 second annealing of the sample in vacuum at 700°C. We also have verified the mechanical change in a contact caused by heating: to move the tube after heating required considerably larger applied force.

Usually an atomic force microscope (AFM) is used for imaging surface topography with a tip that has a radius of curvature down to 10 nm. However, it can also be used to move small objects along the substrates. We have developed an AFM based manipulation method where both moving and imaging are done in the non-contact mode.[22] In this mode one probes the attractive van der Waals force between the vibrating AFM tip and the surface. Using our method, the location of the object can be seen during the movement by monitoring the cantilever oscillation amplitude. This is how we can build electrical circuits containing several nanotubes, or move nanotubes on top of gold electrodes.

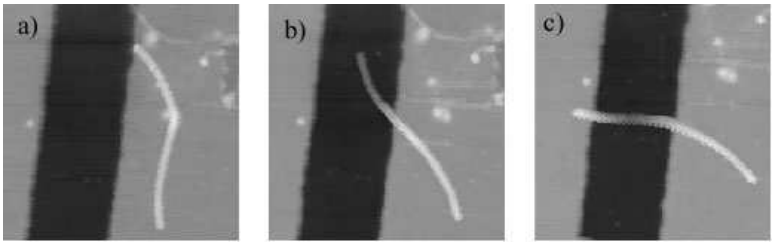

Figure 2: A sequence of AFM-images illustrating smooth bending of a CVD-synthesized tube (length 1.3 μm) during manipulation. According to Figs. 2b and 2c, the tube is in contact with the SiO_2 substrate during the translation process across the gap between the 25 nm thick gold electrodes.

The differences between the arc-discharge and CVD tubes become clearly visible in our AFM manipulations of these tubes. When an AD tube is pushed with an AFM tip, it usually either moves as a whole, without bending, or bends sharply at a certain point, with the rest of the tube staying on its place. These conclusions are similar to those of Falvo *et al.* [23], who studied manipulation of AD tubes more extensively. We have found that manipulation of those CVD tubes that have significant 3D bending out of the surface is very difficult due to the sticking of the tubes to the AFM tip. Also the van der Waals forces that hold the nanotube in place and stabilize strained configurations are reduced. The manipulation of the CVD tubes is also different in the sense that the bending is continuous, without any pivot points, as shown in the manipulation sequence of a CVD tube in Fig. 2. This is of course expected due to the smaller stiffness of CVD tubes. Thus, only manipulation of AD tubes is convenient, when the required distance is several micrometers.

Bending of a nanotube will cause major local changes in the electronic structure, and consequently in intratube transport, as has been shown in calculational work.[24] These references, however, deal basically with single shell nanotubes. On the experimental side, a large increase in resistance has been observed for SWNTs upon bending [25]. For MWNTs, the effect of bending is quite small compared to the total conductance of the tube, as found by Paulson *et al.*[26]

To observe the effect of bending to the resistance of a nanotube, resistance measurements can be done *in-situ* under the AFM. We have, for

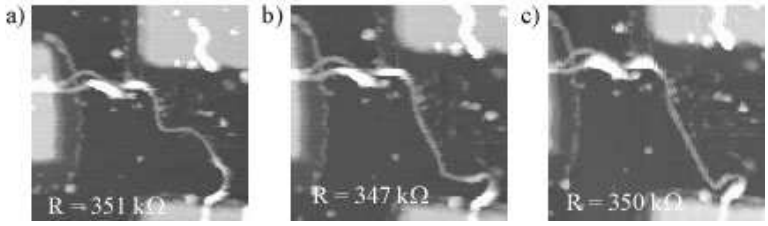

Figure 3: The change in shape of a 1.7 μm long CVD nanotube has only a small effect on the conductance. The measured resistance is marked in each frame.

example, studied one sample, where a MWNT (of length 1.7 μm) is below the electrodes (Fig. 3). The tube is CVD synthesized, as can be seen from its shape. During a long sequence of small movements, we observed no dramatic changes: the resistance varied between 340 and 380 kΩ, the initial value. Both increase and decrease of resistance, typically a few kΩ, was observed between adjacent configurations. Based on our experience on CVD tubes, we expect that a sizable share of the resistance is in the tube itself. Thus we conclude that modest bending of a CVD grown MWNT has only a small effect on the intratube resistance. The result becomes more general when we note that similar conclusions were obtained[26] for AD grown MWNTs. It is not surprising that it is more difficult to bend a multiwalled than a single walled tube so sharply that a tunnel junction would emerge at the site of bending.

4 EXAMPLES OF SETs MADE OF MWNT

We have fabricated MWNT-SETs both from CVD and AD tubes, some of which are shown in Figure 4. Main characteristics of the samples are given in Table 1. The nanotubes had typical diameters of 20 nm for the CVD tubes and 15 nm for the AD tubes. The length of the tube between the electrodes was 0.3-5 μm for the CVD and 0.3-1.7 μm for the AD tubes. Two of the CVD tubes were etched in a RIE process for 15 seconds which reduced their diameter uniformly from 20 nm to 10 nm. The electrodes were either fabricated on top of the tubes (CVD1-CVD3 and AD1) or the tubes were placed on top of prefabricated electrodes (CVD4, AD2 and AD3). The

Table 1: Basic characteristics of our samples. The labeling indicates the nanotube synthesis method. The length L refers to the length between the electrodes. Zero-bias resistances are given for two point configuration at $T = 300$ K and 4.2 K. The small ratio of $R(4.2\text{ K})/R(300\text{ K}) = 1-7$ indicates that our samples are metallic except for AD2 which is semiconducting.

Sample	Comment	R(300 K)	R(4.2 K)	L (μm)
CVD1		230 kΩ	1.6 MΩ	5.3
CVD2	RIE	23 kΩ	31 kΩ	0.3
CVD3	RIE	149 kΩ	190 kΩ	1.5
CVD4		50 kΩ	91 kΩ	0.5
AD1	Cross	71 kΩ	170 kΩ	1.7
AD2		5 MΩ	$\sim$ 200 MΩ	0.3
AD3		28 kΩ	84 kΩ	0.3

electrodes were always made of gold with a chromium sticking layer.

The quality of results obtained on our devices varied over a broad range. The results on CVD tubes were, in general, more irregular than those on AD tubes. Some of the AD tubes turned out to be excellent islands for SETs. As we will show below, the geometrical structure and the construction method have a clear influence on the results.

4.1 Standard CVD-tube device

Figure 4(a) shows an AFM image of device CVD1. It is made of a 6.8 μm long tube which has 25 nm thick gold electrodes evaporated on top of it. At room temperature, the resistance of the tube was 200 kΩ. Below 4 K a zero-bias gap due to Coulomb blockade became clearly visible.

A few gate modulation curves of this MWNT, measured at $T = 0.8$ K, are shown in Fig. 5. Instead of the expected Coulomb blockade period of 1V (estimated for the employed side-gate placed a few μm away), only non-regular gate-modulation traces were found. This irregular behavior points to the formation of a series of intra-tube quantum dots, caused by disorder. Disorder-induced splitting of a tube into several separate islands has been suggested by McEuen *et al.*[27] to explain similar experimental results in SWNTs. From the data set of Fig. 5 and other sets like it, we conclude

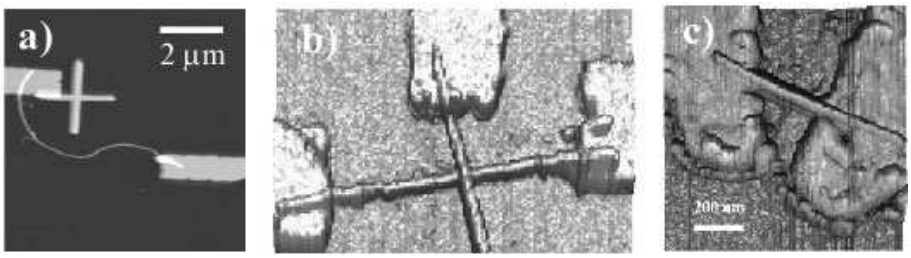

Figure 4: AFM images of some of our samples: a) CVD1 (Image size 7×7 μm^2), b) AD1 with two crossing multiwalled tubes ($\sim$ 1.3×2.4 μm^2), and c) AD3 with a free-standing section of 0.3 μm. Gate leads (not visible in the figures) of the same width as the other electrodes end at a distance of $1-5$ μm from the nanotube island.

that CVD tubes, at least with the present amount of disorder, are not very suitable for central islands of SET electrometers.

4.2 Arc-discharge tubes: Tube-gated device

In contrast to CVD-tube devices, SETs based on AD tubes display regular IV-curve modulation with respect to the gate voltage. Such regularity is particularly nicely illustrated by the results on the device of Fig. 4b (AD1).[28] This sample is in fact composed of two crossing MWNTs: the lower tube, which acts as the central island of the SET, is 2.3 μm long, and the crossing upper tube has been pushed into its position with AFM manipulation. The two-point (zero-bias) resistance over the crossing was $\sim$ 10 MΩ, which increased to $\sim$ 1 GΩ below 4 K. Thus, we could utilize the upper tube for gating the current in the lower tube in this construction. The device has a room temperature resistance of 71 kΩ. A Coulomb blockade develops fully only at subkelvin temperatures, with a gap of about 1 mV at 150 mK. Figure 6 shows the source-drain current I as a function of the source-drain bias voltage V_b and the gate voltage V_g, applied to a separate side gate.

In general, Fourier analysis of the gate modulation curves revealed only one period, indicating the existence of only one island. In contrast to CVD tubes, we conclude that this tube is not broken into sections, neither by defects nor by the other MWNT placed on top of it.

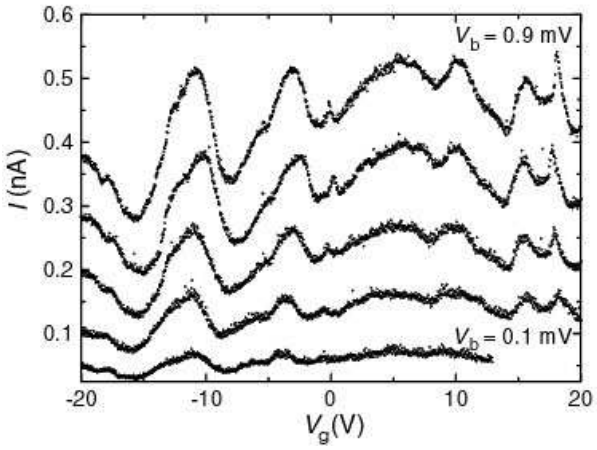

Figure 5: Gate modulation curves (source-drain current I *vs.* gate voltage V_g) measured on the sample CVD1 at $T = 0.8$ K. The bias voltage V_b has been varied from 0.1 mV to 0.9 mV in steps of 0.2 mV.

The gate modulation period with the upper tube as a gate was measured as $\Delta V_g = 4$ mV (using side gate $\Delta V_g = 440$ mV). The tube had a maximum modulation of 8 nA/e. We calculate the gate capacitance to the upper tube as $C_g = e/\Delta V_g = 40$ aF (for side gate $C_g = 0.4$ aF). The present configuration with a crossing nanotube as a large-capacitance gate electrode might be useful in certain SET applications for reducing cross-talk between the gate and the other electrodes. Furthermore, since the voltage gain of a current-biased SET is C_g/C_Σ such a construction allows for devices with high voltage gain [29]. Here C_Σ refers to the total island capacitance including the tunnel junctions.

4.3 AD tubes: 4.2-Kelvin device

Short pieces of nanotubes, equipped with small contact areas, provide a straightforward way to reach SETs with large Coulomb energies. Figure 4c shows one of the shortest nanotube devices (AD3) that we have made from AD tubes. In our short structures, the tubes have been manipulated on top of gold electrodes (AD2 and AD3). The length of the tube between the electrodes is 0.3 μm for both AD2 and AD3. Furthermore, the latter is

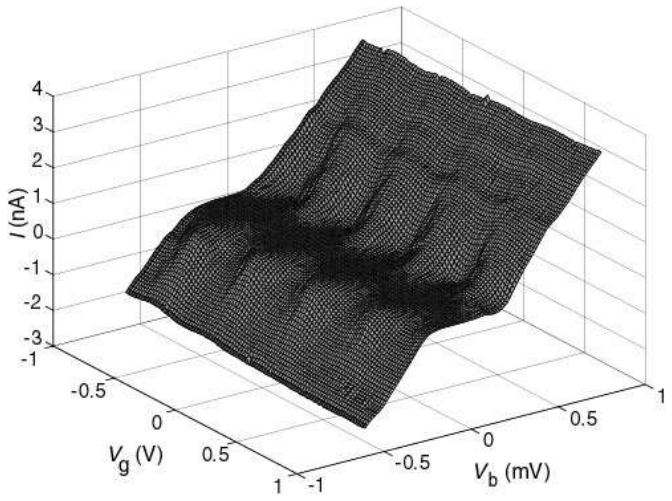

Figure 6: Source-drain current I of the lower tube in sample AD1 at $T = 0.15$ K.[28] The source-drain bias voltage is denoted by V_b and the gate voltage by V_g. The SET blockade region is seen as the rhombic pattern in the center.

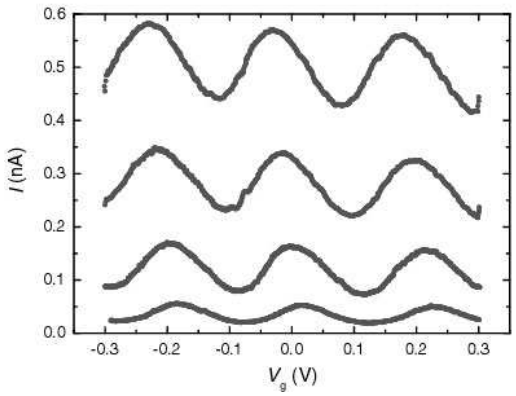

Figure 7: Gate modulation curves measured on sample AD2 at $T = 4.2$ K. Bias voltages are 8.0, 9.9, 11.6, 13.7 mV (from bottom to top).

not touching the substrate between the electrodes. It is separated from the underlying SiO_2 by 17 nm.

The room temperature resistance of AD2 was rather high, 5 MΩ, due to weak gold-nanotube contacts, and increased to ~ 200 MΩ at 4.2 K. Coulomb blockade effects became clearly observable below a few Kelvin. Figure 7 shows gate modulation of the source-drain current at 4.2 K. The modulation period is 200 mV, giving a gate capacitance of 0.8 aF. From measurements of the constant current curves we obtain the junction capacitances and for the charging energy $E_c = e^2/2C_\Sigma = 2.1$ meV. Thus this device is a rather simple implementation of a SET working at the relatively high temperature of 4.2 K. Moreover, scaling down the dimensions should be straightforward in order to minimize the island size and, consequently, to raise the operating temperature even further. The low temperature behavior of sample AD2 has been described by Roschier *et al* [30].

4.4 AD tubes: Low-noise device

Nanotubes are quite susceptible to noise caused by charge trapping to surface states.[31] Multiwalled tubes, fortunately, are not as sensitive in this respect as single walled tubes even though some of our MWNT samples do show quite high noise levels. We obtained the lowest charge noise in device AD3

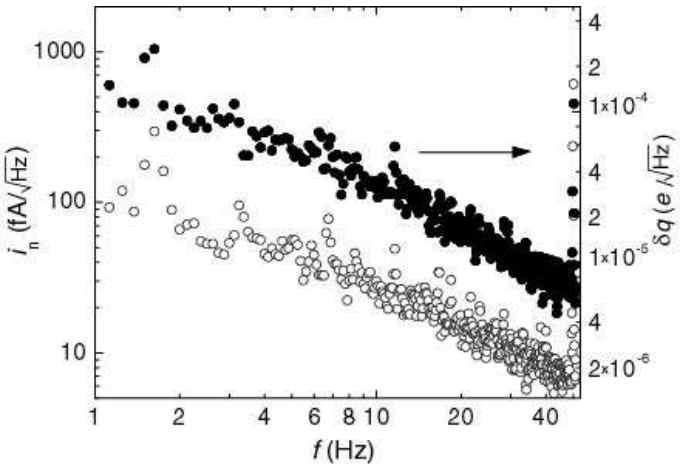

Figure 8: Current noise i_n measured on sample AD3 at $T = 0.15$ K;[32] equivalent background charge fluctuation δq is given on the right scale. Open circles denote the amplifier noise in the measurement setup.

which had extraordinary properties in several respects when compared with our other samples[32]. Especially, the transport in this tube was close to ballistic, which may be the reason behind its good noise properties.

Sample AD3 had a room temperature resistance of 28 kΩ. At sub-kelvin temperatures, we measured a total resistance of $\approx$ 40 kΩ outside the Coulomb blockade regime. The junction resistance of the nanotube-Au contacts are thus less than the quantum of resistance $R_Q \approx 26$ kΩ, which means that the Coulomb blockade cannot fully develop. Consequently, the Coulomb oscillations that we measure are smoothened.[32]

As opposed to the usual Coulomb blockade, nanotube AD3 exhibited increased conductance around zero bias, which we attribute to resonant tunneling. Only two weakly quantized steps are seen, and therefore this tube cannot be said to be fully ballistic. The ballisticity of freestanding samples is likely to be enhanced most by the decreased capacitive coupling between impurity states of the substrate and the MWNT.

Current noise i_n of AD3, measured at a small voltage bias of 70 μV, is displayed in Fig. 8. Frequency dependence of the noise power (i_n^2) has a $1/f^2$ character over the range $5 < f < 50$ Hz. The input equivalent charge noise

q_n is obtained from the measured current noise according to the formula $q_n = C_g i_n/(\partial I/\partial V_g)$. In the Coulomb blockade regime a modulation of the noise was seen as expected for a SET. At a frequency of 45 Hz, we obtain the charge noise $q_n = 6 \cdot 10^{-6}\ e/\sqrt{\text{Hz}}$, which is comparable to the best metallic SET devices reported to date [33]. Theoretically the minimum noise level for a SET is $q_n^{min} = \sqrt{\hbar C_\Sigma \Delta f R_Q/R_T}$, where Δf denotes the frequency range and R_T is the tunneling resistance [34]. Taking $R_Q/R_T \sim 1$ and assuming no cotunneling, we obtain the minimum noise as $1 \cdot 10^{-6} e/\sqrt{\text{Hz}}$. This implies that white noise would dominate over $1/f$ noise above 3 kHz. In fact, the shot noise limited region has been reached in our most recent experiments.[35]

5 MWNTs AS RESISTORS

According to simple Drude-type arguments, disordered MWNTs are good candidates for lumped resistive elements. As was already mentioned above, we have tried to pursue this idea by selecting a couple of CVD tubes for RIE-etching in order to enhance the amount of disorder in them. The etching halved uniformly the diameter from 20 nm to 10 nm. Gold electrodes were placed on top of these tubes. The distance between them is 0.3 μm. Figure 9 shows the IV characteristics of one of these tubes (CVD2) at low temperatures, compared with an untreated CVD-tube (CVD4) that has roughly the same electrode spacing. At room temperature we measure a 2-point resistance of 23 kΩ in the RIE-etched tube. At $T = 100$ mK we observe only a weak Coulomb blockade-type nonlinearity in the IV characteristics and no discernible Coulomb oscillations, in contrast with CVD4. We therefore assume a relatively small contact resistance and consequently that the measured 2-point resistance indicates the intrinsic resistivity of the RIE-etched MWNT to be rather large, on the order of 100 kΩ/μm.

These results were confirmed in our second RIE-etched sample (CVD3), measured in a 4-point configuration. With this sample we observed, in addition, that the resistance measured between different electrode pairs scales roughly with the distance, in accord with Ohmic behavior. Presently we can not tell exactly what role the RIE treatment had for the electronic properties of these tubes. Their intrinsic resistance seems to be higher than that of the untreated CVD tubes by a factor $\simeq 3$.

The high intrinsic resistance together with Ohmic addition rule for the nanotube resistance makes the RIE-etched CVD tubes simple nanoscale

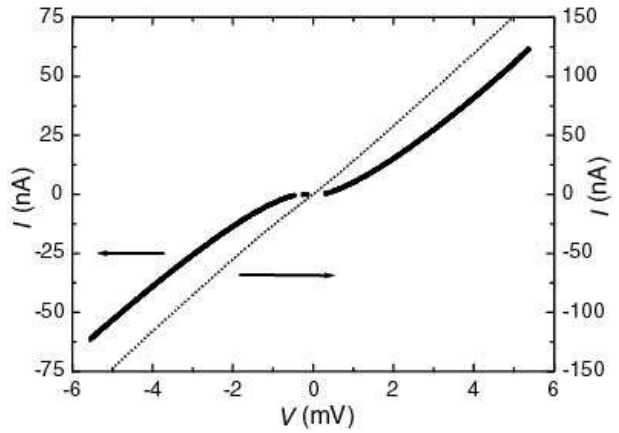

Figure 9: IV-curves for samples CVD2 (right current scale) and CVD4 (left current scale) illustrating the enhanced Ohmic behavior of CVD2 after the RIE treatment. Measurement temperature for both traces was $T = 0.15$ K.

Ohmic resistors. These resistors perform rather well compared with the standard technology utilizing thin chromium films [36]. Typical thin Cr-wires can be employed as linear resistances up to values 10 kΩ/μm while RIE-etched tubes yield 100 kΩ/μm if their small nonlinearity in the zero-bias region can be accepted. With better metal-tube contacts, this non-linearity can presumably be made even smaller.

6 MWNTs AS TRANSMISSION LINES

In the previous sections (Sects. 4 and 5) we treated MWNTs as lumped elements of simple electronic circuits. Howewer, their high aspect ratio allows for nanotube lengths up to macroscopic dimensions. Thus any longer section of a MWNT and nearby metallic structures form a transmission line, where the nanotube acts as an inner conductor. Because the electrons move nearly ballistically in a metallic defect-free tube, one naively expects MWNTs to be excellent transmission lines for high frequency electromagnetic waves. However, rather the opposite turns out to be true, since MWNTs form special, high impedance transmission lines with a low propagation velocity [13].

In an ordinary coaxial cable the electromagnetic wave propagates be-

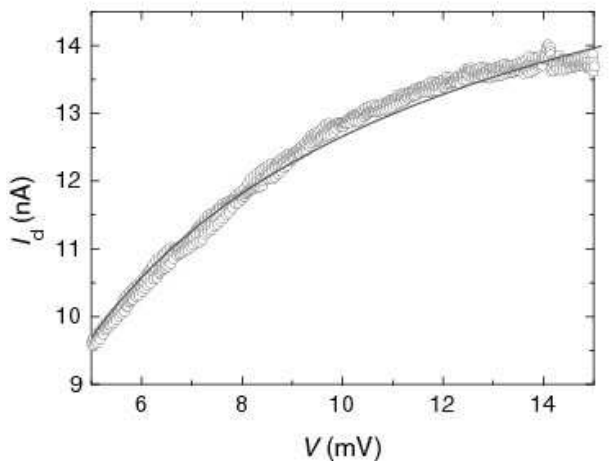

Figure 10: Deficit current $I_d = V/R_T - I$ as a function of voltage V, illustrating the asymptotic approach towards Ohm's law in sample AD1 at $T = 0.12$ K.

tween the metallic outer and inner conductors. The propagation velocity and the impedance of the wave are determined by the electromagnetic inductance and capacitance, with $v_0 = 1/\sqrt{lc}$ and $Z = \sqrt{l/c}$. They are close to the propagation velocity and impedance of electromagnetic waves in free space. In an ordinary coaxial cable, the main part of the inductive energy is stored in the magnetic field induced by the moving electrons. In contrast, in nanotubes the kinetic energy of electrons exceeds their magnetic energy and the inertia of the electrons slows down the electromagnetic waves. The large kinetic inductance l_{kin} is a consequence of the low electron density of the nanotubes.

The electromagnetic waves traveling along nanotubes are actually electron density waves propagating in one dimension, that is, 1D plasmons. If the MWNT is regarded as a transmission line, then its impedance will determine the current-voltage characteristics for electron tunneling into the tube over a mesoscopic tunnel junction, as described by the environmental quantum fluctuations theory.[12, 37, 38] At low voltages, $I \propto V^{\alpha+1}$, where $\alpha = 2Re(Z)/R_Q$. At high voltages, the tunnel junction capacitance C_T starts to shunt the environmental impedance Z, and the power law turns

gradually into an Ohm's law with a characteristic asymptotic region described by a $1/V$-type of tail.[13]

Figure 10 illustrates the asymptotic approach of the IV-curve of sample AD1 towards Ohm's law. We plot in Fig. 10 the deficit current $I_d = V/R_T - I$ which is the deviation of the measured current I from the Ohmic value given by V/R_T. The solid line illustrates the fitting of the theoretical $1/V$-tail: $I_d = \frac{R_Q}{Z}\left(\frac{e}{2\pi C_T}\right)^2 \frac{1}{V}$, which yields for this tube a typical value of $Z = 2.7$ kΩ. Assuming $C = 70$ aF/μm, in fact deduced from the Coulomb blockade offset of the same fits, we obtain $l \sim 0.5$ nH/μm. This inductance value is much higher than expected for magnetic inductance ($l \sim 0.1$ pH/μm) but quite well in agreement with our estimate for the kinetic inductance:[13] $l_{kin} \sim 10$ nH/μm for $M = 4$. We thus conclude that, due to the large kinetic inductance, the propagation velocity in MWNTs is about 1000 km/s and the impedance is on the order of a few kΩ.

7 SUMMARY AND PROSPECTS

Carbon nanotubes vary considerably in size and properties. Restricting this variation to normal-sized AD and CVD multiwalled nanotubes, we presented in the preceding sections our work on different device configurations that can be realized from MWNTs. The difference in structural quality between AD and CVD tubes was discussed, concluding that AD tubes were preferable from the point of view of device physics. We have demonstrated the use of multiwalled carbon nanotubes as nanoelectronics building blocks such as SETs, resistors and transmission lines. Our SET made of two MWNTs demonstrated the feasibility of more complex circuits. Under proper conditions, such as separating the tube from the substrate, it is possible to minimize the noise level and, in other aspects as well, to approach the theoretical limits of performance. On the other hand, our present understanding of MWNTs as transmission lines implies that their kinetic inductance severely limits the propagation speed in them. Nevertheless, the great variety of device structures that can be made from carbon nanotubes suggest that they are among the most promising materials for future molecular electronics.

ACKNOWLEDGMENTS

We acknowledge F. Hekking, E. Sonin, and A. Zaikin for interesting discussions. This work was supported by the Academy of Finland and by the

Large Scale Installation Program ULTI-III of the European Union (HPRI-1999-CT-00050).

References

[1] S. Iijima, *Nature* **354**, 56 (1991).

[2] N. Hamada, S. Sawada, and A. Oshiyama, *Phys. Rev. Lett.* **68**, 1579 (1992); J. W. Mintmire, B. I. Dunlap, and C. T. White, *Phys. Rev. Lett.* **68**, 631 (1992).

[3] T. W. Ebbesen and P. M. Ajayan, *Nature* **358**, 220 (1992).

[4] L. Langer, V. Bayot, E. Grivei, J.-P. Issi, J. P. Heremans and C. H. Olk, L. Stockman, C. Van Haesendonck, and Y. Bruynseraede, *Phys. Rev. Lett.* **76**, 479 (1996).

[5] For a recent review see, *e.g.*, "Special Issue on Nanotubes" in *Physics World*, June 2000, p. 29.

[6] S. J. Tans, M. H. Devoret, H. Dai, A. Thess, R. S. Smalley, L. J. Geerlings, and C. Dekker, *Nature* **386**, 474 (1997); S. J. Tans, A.R.M. Verschueren, and C. Dekker, *Nature* **393**, 49 (1998).

[7] M. Bockrath, D. H. Cobden, P. L. McEuen, N. G. Chopra, A. Zettl, A. Thess, and R. E. Smalley, *Science* **275**, 1922 (1997).

[8] T.A. Fulton and G.J. Dolan, *Phys. Rev. Lett.* **59**, 109 (1987).

[9] For a pedagogical discussion, see *e.g.*, R. Saito, G. Dresselhaus, and M. S. Dresselhaus, *Physical Properties of Carbon Nanotubes*, (Imperial College Press, London, 1998).

[10] P.R. Wallace, *Phys. Rev.* **71**, 622 (1947).

[11] C. Schönenberger, A. Bachtold, C. Strunk, J.-P. Salvetat, and L. Forro, *Applied Physics A* **69**, 283 (1999); A. Bachtold, C. Strunk, J.-P. Salvetat, J.-M. Bonard, L. Forro, T. Nussbaumer, and C. Schönenberger, *Nature* **397**, 673 (1999).

[12] E.B. Sonin, this volume.

[13] R. Tarkiainen, M. Ahlskog, J. Penttilä, L. Roschier, P. Hakonen, M. Paalanen, and E. Sonin, cond-mat/0104019.

[14] A. Bachtold, M. de Jonge, K. Grove-Rasmussen, P.L. McEuen, M. Buitelaar, and C. Schönenberger, cond-mat/0012262.

[15] R. Egger and A.O. Gogolin, cond-mat/0101246.

[16] V. Ivanov, J. B. Nagy, P. Lambin, A. Lucas, X. B. Zhang, X. F. Zhang, D. Bernaerts, G. Van Tendeloo, S. Amelinckx, and J. Van Landuyt, *Chem. Phys. Lett.* **223**, 329 (1994).

[17] K. Hernadi, A. Fonseca, D. Bernaerts, J. B. Nagy, A. Fudala, and A. A. Lucas, *Zeolites* **17**, 416 (1996).

[18] X. B. Zhang, X. F. Zhang, D. Bernaerts, G. Van Tendeloo, S. Amelinckx, J. Van Landuyt, V. Ivanov, J. B. Nagy, Ph. Lambin, and A. A. Lucas, *Europhys. Lett.* **27**, 141 (1994).

[19] J.-P. Salvetat, A. J. Kulik, J.-M. Bonard, G. A. D. Briggs, T. Stöckli, K. Méténier, S. Bonnamy, F. Béguin, N. A. Burnham, and L. Forró, *Adv. Mater.* **11**, 161 (1999).

[20] A. Bachtold, M. Henny, C. Terrier, C. Strunk, C. Schönenberger, J.-P. Salvetat, J.-M. Bonard, and L. Forró, *Appl. Phys. Lett.* **73**, 274 (1998).

[21] Jeong-O Lee, C Park, Ju-Jin Kim, Jinhee Kim, Jong Wan Park, and Kyung-Hwa Yoo, *J. Phys. D: Appl. Phys.* **33**, 1953 (2000).

[22] M. Martin, L. Roschier, P. Hakonen, Ü. Parts, M. Paalanen, B. Schleicher, and E. I. Kauppinen, *Appl. Phys. Lett.* **73**, 1505 (1998).

[23] M. R. Falvo, R. M. Taylor, A. Helser, V. Chi, F. P. Brooks Jr, S. Washburn, and R. Superfine, *Nature* **397**, 236 (1999).

[24] See, *e.g.*, C.L. Kane and E.J. Mele, *Phys. Rev. Lett.* **78**, 1932 (1997); A. Rochefort, Ph. Avouris, F. Lesage, and D.R. Salahub, *Phys. Rev B* **60**, 13824 (1999); M. Buongiorno Nardelli and J. Bernholc, *Phys. Rev. B* **60** , R16338 (1999).

[25] H. Postma, M. de Jonge, Z. Yao, and C. Dekker, *Phys. Rev. B* **62**, 10653 (2000).

[26] S. Paulson, M. R. Falvo, N. Snider, A. Helser, T. Hudson, A. Seeger, R. M. Taylor, R. Superfine, and S. Washburn, *Appl. Phys. Lett.* **75**, 2936 (1999).

[27] P.L. McEuen, M. Bockrath, D.H. Cobden, Y.-G. Yoon, and S. Louie, *Phys. Rev. Lett.* **83**, 5098 (1999).

[28] M. Ahlskog, R. Tarkiainen, L. Roschier, and P. Hakonen, *Appl. Phys. Lett.* **77**, 4037 (2000).

[29] See, *e.g.*, E.H. Visscher, S.M. Verbrugh, J. Lindeman, P. Hadley, and J.E. Mooij, *Appl. Phys. Lett.* **66**, 305 (1995).

[30] L. Roschier, J. Penttilä, M. Martin, P. Hakonen, M. Paalanen, U. Tapper, E. Kauppinen, C. Journet, P. Bernier, *Appl. Phys. Lett.* **75**, 728 (1999).

[31] P.G. Collins, M.S. Fuhrer, and A. Zettl, *Appl. Phys. Lett.* **76**, 894 (2000).

[32] L. Roschier, R. Tarkiainen, M. Ahlskog, M. Paalanen, and P. Hakonen, *Appl. Phys. Lett.*, accepted for publication.

[33] V.A. Krupenin, D.E. Presnov, M.N. Savvateev, H. Scherer, A.B. Zorin, and J. Niemeyer, *J. Appl. Phys.* **84**, 3212 (1998); V.A. Krupenin, D.E. Presnov, A.B. Zorin, and J. Niemeyer, *J. Low Temp. Phys.* **118**, 287 (2000).

[34] A.N. Korotkov, D.V. Averin, K.K. Likharev, and S.A. Vasenko, in *Single-Electron Tunneling and Mesoscopic Physics*, edited by H. Koch and H. Lubbig (Springer, Berlin, 1992), p. 45; A. Korotkov, *Phys. Rev. B* **49**, 10381 (1994).

[35] R. Tarkiainen, M. Ahlskog, L. Roschier, and P. Hakonen, to be published.

[36] J.S. Penttilä, Ü. Parts, P.J. Hakonen, M.A. Paalanen, and E.B. Sonin, *Phys. Rev. B* **61**, 10890 (2000).

[37] M.H. Devoret, D. Esteve, H. Grabert, G.-L. Ingold, H. Pothier, and C. Urbina, *Phys. Rev. Lett.* **64**, 1824 (1990).

[38] G.-L. Ingold and Yu.V. Nazarov, in: *Single Charge Tunneling*, ed. H. Grabert and M.H. Devoret, (Plenum Press, N.Y., 1992), pp. 21-107.